

DETERMINATION OF LYMPHATIC VASCULAR IDENTITY AND DEVELOPMENTAL TIMECOURSE IN ZEBRAFISH (*DANIO RERIO*)

M. Coffindaffer-Wilson, M.P. Craig, J.R. Hove

Department of Molecular and Cellular Physiology (MC-W,MPC,JRH), University of Cincinnati
College of Medicine, and Division of Developmental Biology (MC-W), Cincinnati Children's Hospital
Research Foundation, Cincinnati, Ohio USA

ABSTRACT

*Zebrafish lymphatics have been shown to share a number of characteristics with their human counterparts, making the fish a potentially useful model for studying lymphatic development and disease. The utility of the zebrafish lymphatic model would be substantially enhanced by an improved understanding of the spatiotemporal development of the primary lymphatic vasculature. The goal of this project is to identify and map the major zebrafish lymphatic structures throughout embryonic to early juvenile stages of development. Two transgenic lines, *kdr-l:RASmCherryxfl1:GFP* and *stabilin1:YFP*, were recently derived to assist in the study of developing lymphatic vasculature, but their specificity has not been rigorously tested. In the course of the present study, we experimentally validate the utility of these two marker lines as potential tools for establishing lymphatic vascular identity and visualizing developmental lymphangiogenesis. We introduced twenty nanometer red fluorescent microspheres into the blood vasculature of *fl1:GFP* zebrafish and collected tiled optical z-sections at time intervals spanning early development. Three-dimensional reconstructions of the vasculature were used to differentiate between blood and lymphatic vessels. Age-matched injected embryos were compared to the two transgenic lines to*

*further assess their specificity. We created a spatiotemporal map of the major lymphatic vessels in the developing zebrafish including a previously unidentified lymphatic vessel in the gastrointestinal tract. We conclude that the *kdr-l:RASmCherryxfl1:GFP* line accurately identifies developing lymphatic vessels with the exception of those associated with the gastrointestinal tract. The *stabilin1:YFP* line, however, is less reliable, as it marks both venous vessels and lymphatic vessels.*

Keywords: zebrafish, lymphangiogenesis, angiography, suprainestinal lymphatic, LECs, vasculature

The lymphatic system plays an important role in immune cell trafficking, tissue fluid homeostasis, and absorption of dietary fats. Prior studies suggest that lymphatic vessel growth, termed lymphangiogenesis, may have a central role in several clinically relevant pathologic disorders, including inflammation, obesity, hypertension, tumor metastasis, and lymphatic vessel dysfunction (reviewed in 1). Lymphatic vessel malformations lead to impaired immune response and chronic edema, eventually progressing to fibrotic and adipose tissue formation (2,3). Despite its importance, there is inadequate knowledge about the development and maintenance of this critical system. Treatment through physical therapy or surgery may offer modest

quality of life improvements but there are currently no cures for many lymphatic diseases. As a result, there is clearly a critical need for improved understanding of lymphatic biology and the etiology of lymphatic disease.

The most widely recognized model of lymphangiogenesis was proposed by Florence Sabin in 1902. Her study suggested that the cervical lymph sacs bud from the cardinal vein and spread by endothelial sprouting and remodeling to establish a functional lymphatic system (4). Since that time, research utilizing murine models had been particularly important in establishing what is currently known about normal and pathologic lymphatic biology (reviewed in 3). These studies, however, are limited because direct optical observation of lymphangiogenesis is virtually impossible when the embryonic development occurs *in utero*. In addition, murine studies are both costly and time consuming. As a result, researchers have turned to non-traditional vertebrate models (e.g., fish, amphibians) that offer greater experimental flexibility and lower cost. Recently, the zebrafish (*Danio rerio*) has emerged as one such alternative for the study of lymphangiogenesis (5,6). Embryonic zebrafish are optically transparent, allowing near-complete visual access to developmental lymphangiogenesis as it occurs. Further, the zebrafish lymphatic system shares many of the same molecular, morphological, and functional properties found in the lymphatics of higher vertebrates (6), including the origination of the lymphatic sac from the cardinal veins (7). The genetic tractability of the zebrafish has already been utilized in forward genetic screens to identify potentially important genes regulating lymphangiogenesis (8). The first major lymphatic structure to be discovered in the zebrafish was the thoracic duct (TD) (5,6), which is the primary lymphatic vessel in the fish. More recently, the zebrafish was also found to have intersegmental lymphatic vessels (ISLV) (8,9), as well as a dorsal longitudinal lymphatic vessel (DLLV) (8).

In order to better define the strengths and limitations of the zebrafish as a model for understanding human lymphangiogenesis, it is necessary to know when and where the major lymphatic vessels form. With a reliable spatiotemporal map of normal lymphatic development as a foundation, researchers will be better able to utilize the zebrafish model to probe the functional and genetic foundations of lymphatic development. In addition, a reliable method for determining vessel identity (e.g., lymphatic vs blood vascular) is necessary as misidentification of early embryonic vessels is not uncommon and may confound conclusions of vessel origin. The data presented in this paper address both of these needs by: i) creating a detailed structural map of major lymphatic vessels from 2 days post fertilization (dpf) through the early juvenile stage, and ii) evaluating the accuracy of two recently derived fluorescent transgenic lines, Tg(*kdr-l:HsHRAS-mCherry*)s916x*fli1:GFP* and Tg(*stabilin1:YFP*)^{hu4453}xTg(*casper*)^{b286}, used for lymph vessel identification and visualization (8). In addition to providing a baseline for normal lymphatic development, these data should also prove useful in discussions on the mechanisms underlying early migration patterns of lymphatic endothelial cells (LECs) as they form the nascent lymphatic vasculature.

MATERIALS AND METHODS

Zebrafish Models Highlighting Vascular Systems

Three transgenic lines were utilized for this project: *kdr-l:RASmCherryxfli1:GFP* (reported red fluorescent blood vasculature and green blood and lymphatic vasculature), *stabilin1:YFPxcasper* [reported yellow posterior cardinal vein (PCV) and lymphatic vessels], and *fli1:GFP* (with green lymphatic and blood vessels). Additionally, microsphere-based angiography of *fli1:GFP* embryos over the first two weeks of development enabled us to differentiate between blood and

lymphatic vessels to create a spatiotemporal lymph vessel map that then could be used to assess the specificity of the other two transgenic lines.

Care and Maintenance of Zebrafish Embryos

Embryos were obtained from breeding adult zebrafish in the University of Cincinnati-Cincinnati Children's Hospital Medical Center (UC-CCHMC) zebrafish colony. Adult fish are maintained at 28.5°C with 14:10 light:dark cycles and fed a mixed diet of live *Artemia* and Aquatox flake food (Aquatic Ecosystems, Inc.). Raising, maintaining and spawning of adult zebrafish, as well as care of young embryos, was performed as previously described (Westerfield, 1995). Water chemistry was maintained at pH 7.1-7.4, conductivity 490-530 μ S, temperature 26.5-28 5°C and dissolved oxygen of 5.0-7.5 mg L⁻¹. All animal husbandry and experimental manipulations were performed in accordance with both UC and CCHMC IACUC guidelines.

Confocal Imaging

Embryos were mounted on their sides in glass-bottom petri dishes into 1.2% agarose containing 125-150 mg L⁻¹ MS-222 after Hove et al (10). Imaging of the embryonic vasculature was performed using a Ziess LSM 510 scanning confocal scanner and associated Axiovert 100M inverted microscope. Sample illumination was provided by 488 nm and 543 nm solid-state lasers as appropriate for the GFP (488 nm), YFP (513 nm), and RASmCherry (587 nm) fluophores. The light path was configured with a HFT 488/543 excitation filter, a bandpass 500-550 nm IR filter and a longpass 560 nm filter to establish the individual detection channels. A Plan-Apochromat 20X/0.6 objective (zoom 0.7) was used throughout. Tiled Z-stacks (average final image dimensions 512x, 3584y and 30z) of each embryo were taken using a 5 micron Z-plane interval to create three-dimensional

renderings of each fish, unless otherwise noted. The average 3.20 microsecond pixel dwell time corresponded to approximately 20 minutes imaging time per fish. Maximum intensity projection (MIP) images were prepared in Axiovision 4.8.1 (Carl Zeiss Microimaging GmbH, Germany). All images shown are MIPs unless otherwise noted.

Angiography

fli1:GFP embryos (2 dpf through 17 dpf) were injected with 20 nm carboxylate-modified red fluorescent (580 nm λ_{EX} , 605 nm λ_{EM}) FluoSpheres (Invitrogen Inc., Carlsbad, CA) at a final 0.2% solids concentration. Microinjections were performed using a PLI-100 Pico Injector (Harvard Apparatus, Hollister MA) with 2-3 μ m borosilicate glass pipets. Multi-bolus injections were made into the common cardinal vein (CCV) or posterior cardinal vein (PCV) using injection pressures of 2-5 psi. Injected microspheres remained suspended in the circulating blood, including the intersegmental vessels and finer vasculature, but their size prevented paracellular leakage through the blood vascular endothelium and subsequent entry into the interstitium and lymphatic bed throughout the imaging interval (typically <1hour).

Wiring Diagrams

The wiring diagrams detailing the developing lymphatic system were prepared by tracing over representative MIP images of injected *fli1:GFP* embryos with some structures hand drawn when tracing was not possible. The rendering wire diagrams were not averaged, as all *fli1:GFP* injected replicas exhibited only extremely minor collective differences at any given time point which did not warrant averaging. The wiring diagrams were prepared with lymphatic vasculature denoted in green, arterial vasculature in red and venous vessels in blue.

Abbreviations

TABLE 1
Vasculature Nomenclature Abbreviations

aISV: Arterial Intersegmental Vessel	PCV: Posterior Cardinal Vein
CCV: Common Cardinal Vein	SIA: Supra-intestinal Artery
DA: Dorsal Aorta	SIL: Supra-intestinal Lymphatic
DLAV: Dorsal Longitudinal Anastomotic Vessel	SIV: Sub-intestinal Vein
DLLV: Dorsal Longitudinal Lymphatic Vessel	TD: Thoracic Duct
GI: Gastrointestinal	vISV: Venous Intersegmental Vessel
ISLV: Intersegmental Lymphatic Vessel	VTA: Vertebral Artery
PAV: Parachordal Vessel	

Blood and lymphatic vessel abbreviations for vessels found in the zebrafish are included in *Table 1* to provide clarity for the vascular nomenclature used in the Results and Discussion.

RESULTS

Imaging of Transgenic Lines

The GFP tag in the *fli1:GFP* embryos fluorescently labeled both the blood and lymphatic vessel walls. Introduction of red fluorescent microspheres into the blood vasculature labeled all blood vessels (green walls with red lumens) and made it possible to distinguish them from lymphatic vessels (green walls only). Microspheres were injected into the CCV or PCV blood flow and peripheral to the developing lymphatic structures being interrogated in order to minimize disruption to the trunk structures being imaged. Confocal images were reconstructed to create a multidimensional map of the lymphatic vasculature throughout development in the zebrafish and to validate experimentally the accuracy of the *stabilin1:YFP* and *kdr-l:RASmCherryxfli1:GFP* lines. All embryos were oriented in the posterior to anterior view for imaging and a blue scale bar representing 20 μm was added.

LECs Clustering to Form the TD

At 2dpf, we observed that *stabilin1:YFP* transgenic embryos exhibit fluorescent PCV, parachordal vessels (PAVs), and lower

intersegmental vessels (ISVs) (*Fig. 1A*). Clear patches of vascular endothelial (GFP tagged) cells starting to form the TD were evident in both the injected and *kdr-l* embryos just as the LECs had begun to migrate (6) (*Fig. 1B,C*). We also noted patches of endothelial cells forming three distinct vessels dorsal to the TD (*Fig. 2*). These vessels are the vertebral artery (VTA) (1) (which later splits into two vessels) (11); and PAVs (2 & 3), recently referred to as the parachordal lymphangioblast string or PL string (9). These vessels were clearly not lymphatic as they later acquired blood flow at 3.5dpf (confirmed in angiographed embryos and by *kdr-l* fluorescence). Interestingly, the *kdr-l* blood vessel marker was not expressed in the gut blood vasculature at any of the developmental stages analyzed in this study.

Appearance of the DLLV and SIL

The TD was distinguishable from the PCV in *stabilin1:YFP* embryos by 3dpf. YFP also marks the PAVs at this stage and ISV fluorescence was observed more dorsally (*Fig. 3A*). The TD was partially segmented, as shown in the *kdr-l:RASmCherryxfli1:GFP* transgenic line (*Fig. 3B*). While the LEC patches were not entirely coalesced at this stage, the TD is nearly a single continuous structure (confirmed by *fli1:GFP* injected embryo analysis, *Fig. 3C*). The DLLV formed similarly to the TD, by first forming LEC clusters and then filling in to form a continuous vessel (*Fig. 3C*).

Analysis of the GI vasculature revealed a previously unknown lymphatic vessel in 3dpf *fli1:GFP* injected fish (Fig. 3C,D). This supraintestinal lymphatic vessel (SIL) vessel formed from coalescing LEC islands similar to that observed in the TD and DLLV and closely followed the supraintestinal artery (SIA) (ventral to the PCV). The presence of the SIL supports the contention that the lymphatic system of fish likely serves in the absorption and transport of dietary lipids from the GI tract as it does in the systems of higher vertebrates.

Completion of the TD and Continued Coalescence of the DLLV and SIL

At 4dpf, the developing lymphatic bed remained poorly labeled in *stabilin1:YFP* embryos making it difficult to adequately define YFP-positive vessel identities with this line (Fig. 4A). The vessel identities indicated by the *kdr-l:RASmCherryxfli1:GFP* and *fli1:GFP* angiography embryos continued to mirror one another closely, providing a clear delineation of vessel identity in the absence of a line that robustly expresses direct lymphatic labeling (Fig. 4B,C). At this stage, only an occasional gap remained between the TD sections. The forming ISLV were also observed immediately adjacent to the arterial intersegmental vessels (aISV) at 4dpf (Fig. 4C,D). The DLLV and SIL continued their formation out of adjacent LEC clusters (Fig. 4D,E). A cross-sectional view through the zebrafish trunk was derived from a one micron interval z-stack using Improvion Volocity. This unique perspective revealed that the VTA has started to split into two distinct vessels and the two PAVs extend parallel to one another (Fig. 5). This view also revealed that the DLLV continuously intertwined with the dorsal longitudinal anastomotic vessel (DLAV) and that the SIL is located between the SIV and SIA in the plane of the cross-section.

Continued Analysis through the Juvenile

Stages, Lymphatic Vessel Maturation

The 5dpf *stabilin1:YFP* larvae exhibited YFP fluorescence marking the PCV, TD, PAVs, and most of the ISVs, but its weak fluorescence intensity made separation of fluorescently tagged structures from surrounding autofluorescence difficult. At this stage, the TD had developed into a fully continuous structure. The DLLV LECs had completed their dorsal migration and began extending both caudally and rostrally in the process of forming a fully continuous vessel. The ISLVs were the most difficult lymphatic vessels to visualize due to their tight pairing with aISV in the transgenic lines utilized in this study. Nevertheless, the ISLV were visible in *fli1:GFP* injected embryos at this stage (Fig. 6A). Additionally, the SIL vessel was observed as a nearly complete structure intertwined around the SIA near the PCV (Fig. 6B,C).

Little change in the primary vessels of the lymphatic tree occurred between 5 and 6dpf.

The DLLV and SIL, while not yet fully connected, appear to be nearing completion (Fig. 7). ISLVs can be seen at this stage and are still closely positioned to the aISVs (Fig. 7).

Additional analysis of embryos from 10 and 17dpf *fli1:GFP* larvae revealed no evidence of significant lymphatic development, although the DLLV is clearly delineated at day 10 in the *fli1:GFP* injected line (Fig. 8A) and remains unchanged through 17dpf (Fig. 8B). The SIL at 17dpf is fully located between the SIA and PCV (Fig. 8B).

DISCUSSION

Our understanding of normal and pathological lymphatic biology lags far behind that of the blood vascular system and many of the other organ systems; yet, without a functioning lymphatic system, severe disease or death will occur. A properly functioning lymphatic system is necessary for bodily fluid and protein homeostasis, immune regulation,

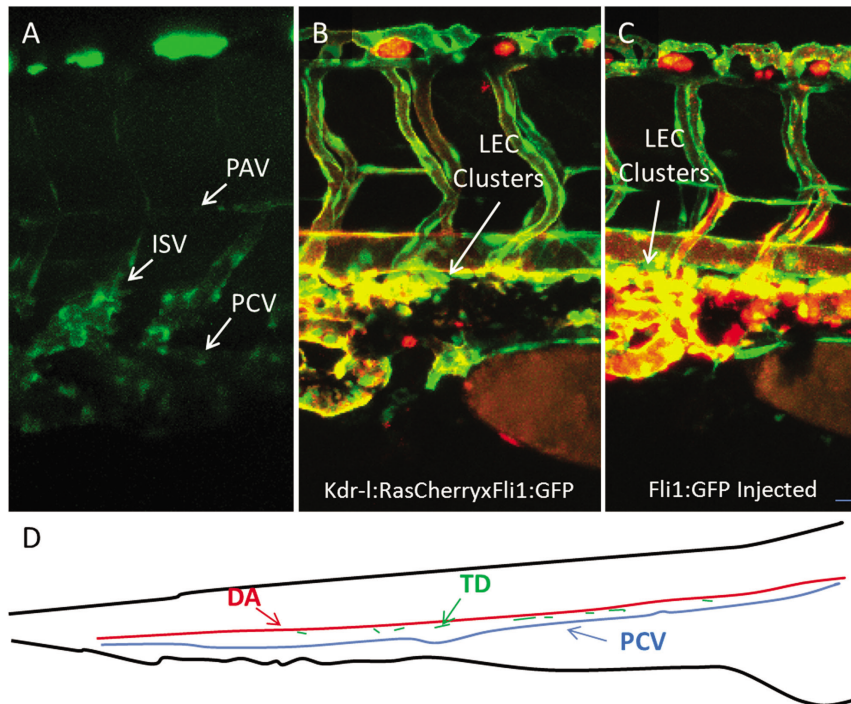


Fig. 1. 2dpf Embryos. A) Stabilin1:YFPxcasper embryos exhibit dim fluorescence from the YFP marker in the PCV, intersegmental, and PAVs. B) Kdr-l:RASmCherryxfli1:GFP embryos closely resemble the fli1:GFP injected embryos, however, they lack *kdr-l* fluorescence in the GI blood vasculature. C) Fli1:GFP angiography embryos depict LEC clusters that have started to form the TD. D) Image rendering at 2dpf reveals isolated islands of LECs coalescing between the DA and PCV where they will form the TD.

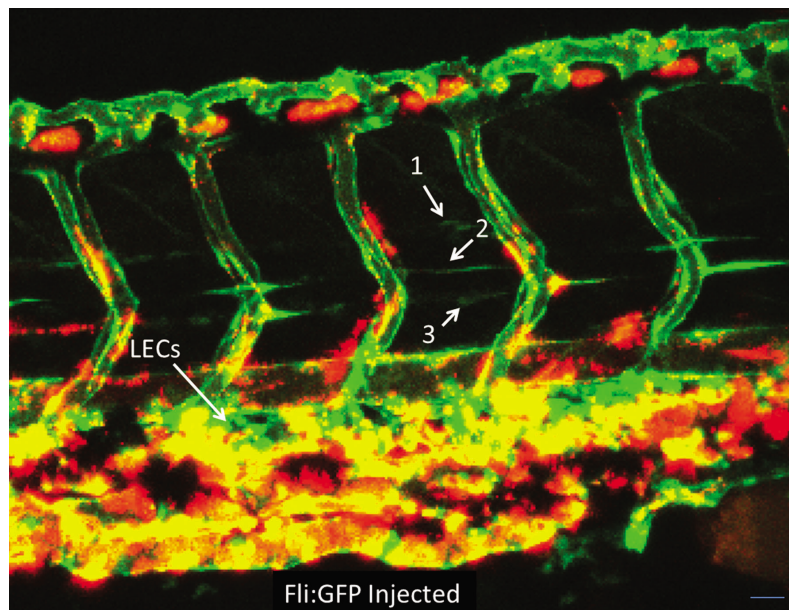


Fig. 2. Fli1:GFP angiograph of 2dpf embryo illustrates the VTA (1) and PAVs (2 & 3).

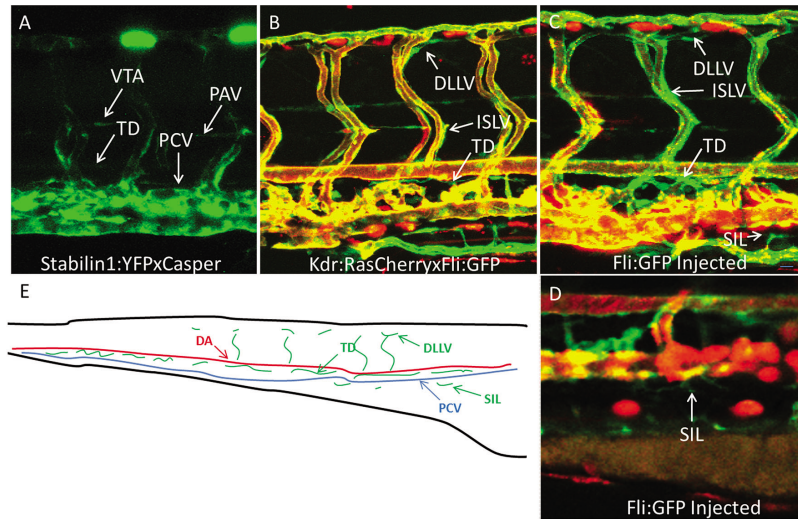


Fig. 3. 3dpf Embryos. A) *Stabilin1:YFPxcasper* embryos exhibit YFP marking the PCV, TD, intersegmental vessels, and PAVs. B) *Kdr-l:RASmCherryxfli1:GFP* embryos show clear TD and DLLV formation marked by only *fli1:GFP* at this stage of development. C) Angiography in 3dpf *fli1:GFP* embryo displays clear green fluorescence in the DLLV, ISLV, TD, and SIL, allowing for easy optical visualization. D) A single plane image in the *fli1:GFP* angiographed embryo reveals the presence of the SIL at 3dpf. E) Model rendering of 3dpf embryo highlights the isolated islands of LECs starting to form the TD, DLLV, and SIL.

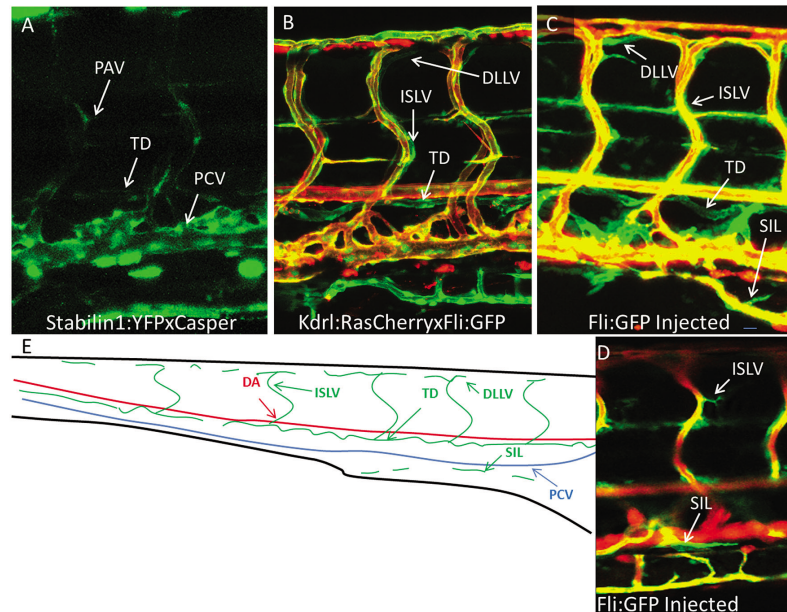


Fig. 4. 4dpf Embryos. A) YFP fluorescence in a *stabilin1:YFPxcasper* embryo marks the PCV, TD, PAVs, and intersegmental vessels at 4dpf. B) A 4dpf *kdr-l:RASmCherryxfli1:GFP* embryo allows visualization of the TD, ISLV, and DLLV at this stage in development. Note that gut blood vasculature remains void of *kdr-l* expression at this stage. C) *Fli1:GFP* angiography clearly shows all major lymphatic structures at 4dpf; these structures includes the TD, ISLV, DLLV, and SIL. D) A single plane image of an angiographed *fli1:GFP* embryo captures formation of the SIL. E) Model rendering of 4dpf embryo highlights the completion of the TD and coalescence of LECs forming the DLLV, and SIL.

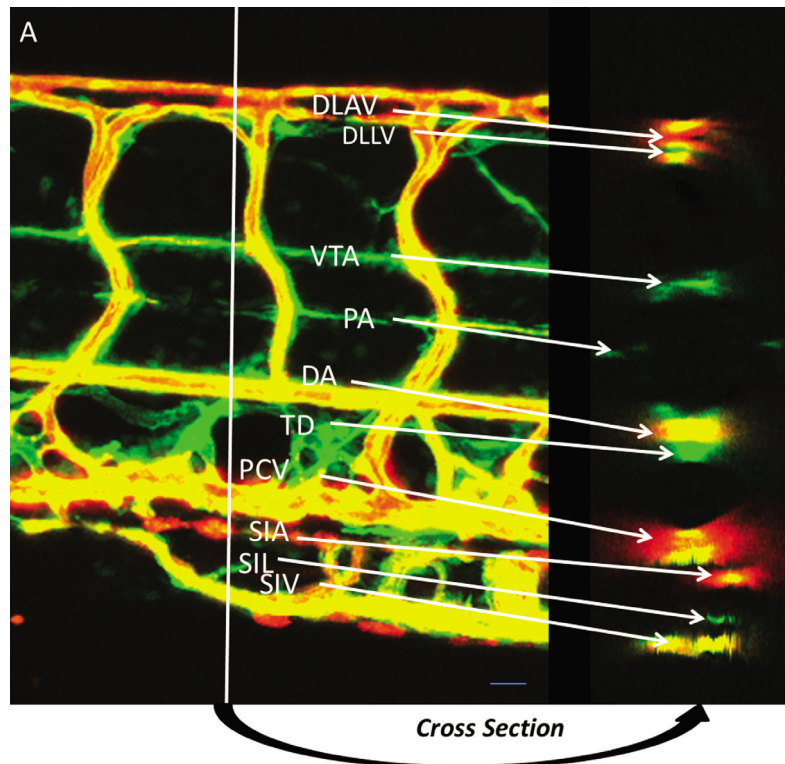


Fig. 5. Three-dimensional reconstruction of an embryonic cross-section for characterization and analysis of vessel locations in the z-plane. This view illustrates both the lymphatic and blood vasculature viewed caudally down the body long axis of a 4dpf *fli1*:GFP fish.

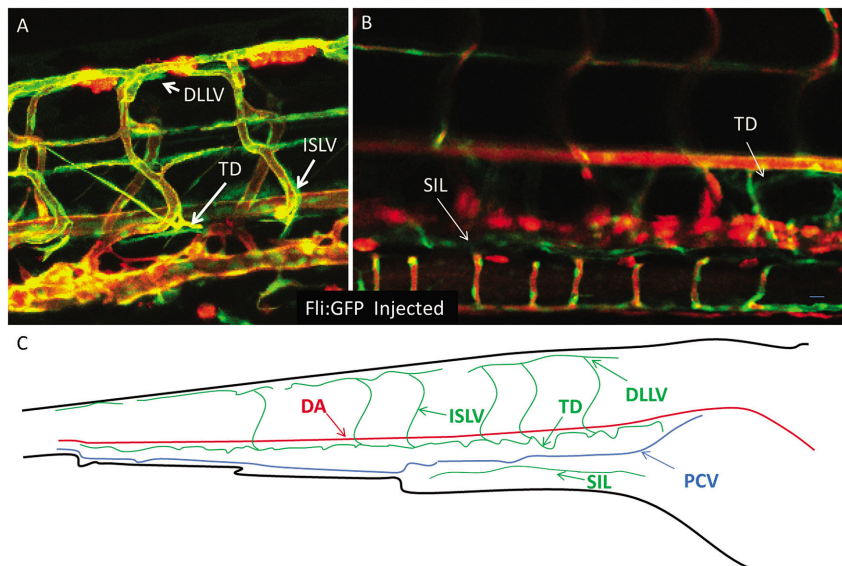


Fig. 6. 5dpf Embryos. A) Angiography of a 5dpf *fli1*:GFP embryo facilitates visualization of the ISLV (marked by an asterisk). B) This single plane image of the *fli1*:GFP injected embryo clearly depicts the SIL. C) A 5dpf model rendering of the major lymphatic structures reveals a complete TD, as well as nearly formed DLLV and SIL vessels.

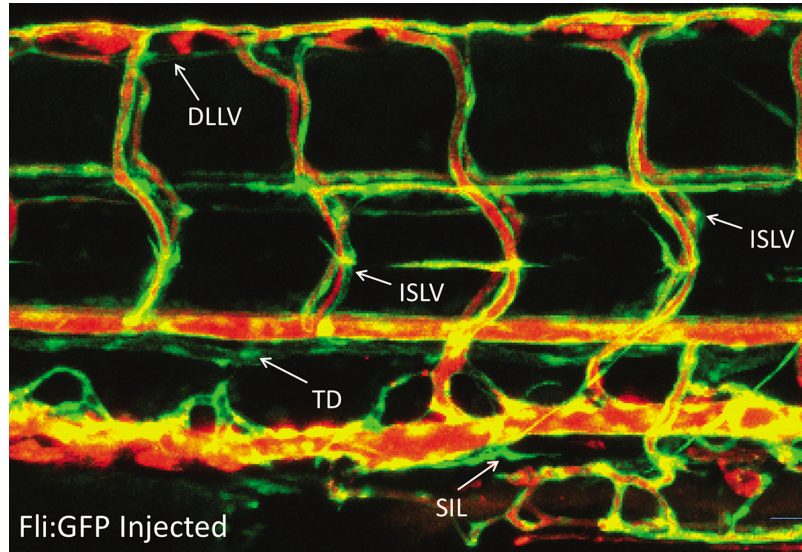


Fig. 7. A 6dpf angiograph of a fli1:GFP embryo illustrating the TD, DLLV, ISLV and SIL.

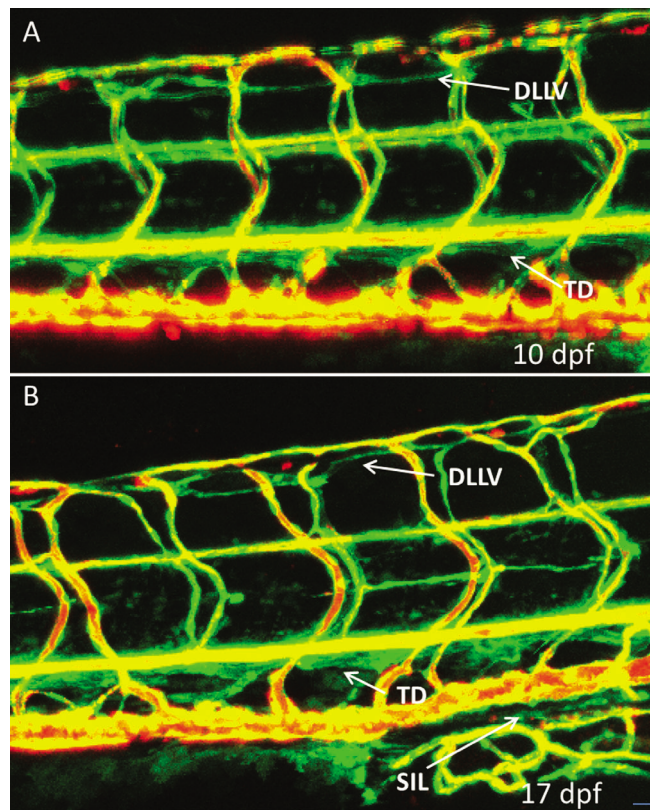


Fig. 8. Fli1:GFP Angiography Embryos. A) At 10dpf, fli1:GFP angiographed embryos do not reveal the development of additional undescribed lymphatic vessels, although thickening of the TD and DLLV are apparent. B) At 17dpf, no additional lymphatic vasculature is observed.

and dietary fat absorption. There are inadequate treatments for diseases of the lymphatic system and seldom cures, leaving patients suffering from lymphatic disease in a generally compromised standard of living.

Murine studies have been instrumental in elucidating much of what has been recently uncovered about normal and pathologic lymphatic biology. While these studies have identified some of the genes involved in the patterning and functional regulation of the lymphatics, they are constrained by the slow development, surgical invasiveness, and poor optical access inherent in larger animal models that develop *in utero*. While a small animal model is needed to advance lymphatic research, comparative phylogenetic analyses reveal that only vertebrates possess a true lymphatic vascular system (12). The frog has been used as a model system for lymphangiogenesis (13), but it has specialized propulsive organs (e.g., lymph hearts, small contractile structures containing striated muscle fibers) (12,14) different from mammalian systems. Fish lymphatic systems lack these lymph propelling organs, making them more analogous to their mammalian counterparts.

The zebrafish first emerged as a model for lymphatic development in 2006 (5,6). These early research efforts revealed that the zebrafish shares many of the lymphatic morphological, molecular, and functional characteristics found in higher vertebrates (5,6). Several useful characteristics have enticed a number of researchers to pursue lymphatic study in the zebrafish model. These include its amenability to intravital imaging, rapid development (TD forms by 4dpf in the fish while maturation into differentiated lymphatic vessels commences at E11.5-E12.5 in the mouse) (3), and genetic tractability. The TD was the first lymphatic vessel described in the zebrafish (5,6). Since then, the DLLV and ISLVs have been identified (8) and, it was recently discovered that zebrafish form a lymph sac (as do humans), and they have both left and right asymmetric collecting ducts (15). Although

these vessels have been identified previously, the spatiotemporal mapping has not been described, making it difficult to identify lymphatic vesicular anomalies in the zebrafish at various early stages.

The first lymphatic molecular studies performed in the zebrafish revealed that genes known to be involved in lymphangiogenesis in mammals were conserved in fish. These studies demonstrated that prospero-related homeobox 1 (PROX1) (6), neuropilin-2 (6), and lymphatic vessel endothelial hyaluronan receptor 1 (LYVE-1) (15) were expressed in both human and embryonic zebrafish lymph vessels and that angiopoietin 2 antibody (5) marks the lymphatic vessels in adult zebrafish. Also conserved is the requirement for VEGF-C signaling for lymphatic development in the zebrafish (5,6). This evolutionary conservation has led researchers to explore the use of the fish model to identify new genes involved in lymphangiogenesis. A recent forward genetic screen identified the *ccbe1* gene as a key regulator in fish lymphatic development (8) and ultimately led to the finding of a link between *ccbe1* mutation and lymphatic hypoplasia in a human disorder (16). New data derived from zebrafish research suggest a link between both synectin (17) and Dll4/Notch (18) signaling during lymphatic development. These and other studies have begun to open the use of the zebrafish model system as a “living assay” for lymphatic therapeutic drug analyses. For example, rapamycin has been shown to inhibit lymphangiogenesis in zebrafish as it does in mammalian systems (15). These powerful new molecular approaches to dissect lymphatic developmental morphology and function should benefit substantially from an improved understanding of the developmental position and time course of zebrafish lymphatic vessels.

The data presented in this paper provide a thorough spatiotemporal map of the formation of key lymphatic vessels in the developing zebrafish which may serve as a foundation for experimental manipulations of

key developmental players. We found that LECs began clustering between the DA and PCV at 2dpf. These LECs arose from the parachordal lymphangioblast string and migrated along aISV beginning at approximately 2dpf (18). A day later, clear LEC sections began to form the TD, DLLV, and SIL. All of these major lymphatic vessels began as clusters of LECs which eventually coalesced to form continuous vessels over time. The TD was completely formed by 4 to 5dpf, and the DLLV and SIL became complete later (5-7dpf).

Our experimental approach facilitated the discovery of a previously undocumented zebrafish GI lymph vessel, the SIL. The presence of intestinal lymphatics further supports the conservation of vertebrate lymphatic development and dramatically expands the potential utility for the zebrafish as a gut lymphatic model for human disease. While the functional role of the SIL will need to be determined empirically, any resulting support for comparisons with the function of human GI lymphatics (lacteals) will serve to energize studies using the zebrafish model for the study of lipid transport. It is conceivable that the zebrafish model system may be potentially useful in addressing questions of lymphatic lipid absorption and deposition in ongoing efforts to uncover the proposed relationship between lymphatic disease and obesity (19).

Experimental validation of angiographed vessels with the two transgenic lines used to visualize lymphatic vessels, *stabilin1:YFPxCasper* and *kdr-l:RASmCherryxfli1:GFP*, helped to clarify the strengths and limitations of both lines. In general, we found that *stabilin1:YFP* exhibited weak fluorescence intensity making it difficult to separate specifically labeled lymphatic structures. Additionally, the *stabilin1:YFP* tag marked venous blood vessels in addition to lymphatic vessels. Taken together, these limitations make the *stabilin1:YFP* line suboptimal for independent identification and visualization of lymphatic vasculature.

Bussmann et al (18) recently created a transgenic line, *SAGFF27C;UAS:GFP*, with higher reporter expression that may replace the *stabilin1:YFP* line. Crossing this line with a *flt1^{enh}:RFP* transgenic line (which allows visual differentiation between aISV and vISV) has the added benefit of more clearly identifying the ISLVs. However, the GFP in *SAGFF27C;UAS:GFP* appears to mark all venous blood vessels as well. Therefore, this newly derived line may experience similar difficulties in conclusively differentiating between blood vessels and lymphatic vessels.

In contrast, the dual fluorescing *kdr-l:RASmCherryxfli1:GFP* line provided a robust means of assigning blood and lymph vessel identities as confirmed by a strong correlation with *fli1:GFP* angiographic determined roles. The only discrepancy between this transgenic and angiographically mapped structures was found in the gut vasculature where the *kdr-l:RASmCherry* expression failed to highlight blood vessels (confirmed by circulation of the red beads in the angiography method) in the GI region of the fish. The lack of *kdr-l* red fluorescence in the GI blood vasculature leaves these vessels only marked by *fli1:GFP*. Therefore, both the blood and lymphatic vasculature are labeled only in green in this region, which does not allow for optical differentiation between the two. This finding is disappointing as the newly discovered SIL can only be clearly visualized through the angiographic method and not through either the *stabilin1:YFPxCasper* or *kdr-l:RASmCherryxfli1:GFP* transgenic lines. In the future, it will be interesting to see whether a LYVE-1 transgenic will be produced to label LECs clearly, as two groups have now used the expression of the gene to determine lymphatic vessel identity (7,20).

In September 2007, the National Institutes of Health convened a trans-NIH working group to address the deficit in understanding of lymphatic biology and made recommendations for future directions in lymphatic research. One of the work-

group's recommendations was to generate and characterize animal models to foster research advances in lymphatic research. The zebrafish model appears to be one such system capable of addressing this deficit. Combining powerful genetic models with emerging imaging technologies should allow lymphatic researchers to circumvent many of the limitations that have hindered progress towards more effective treatments for those who suffer from lymphatic disease.

ACKNOWLEDGMENTS

We would like to thank Matt Kofron, PhD for assisting with image acquisitions and Mitul B. Desai for aid in embryo preparation. *kdr-l:RASmCherry x flil:GFP* fish were generously provided by Didier Stanier, PhD of UCSF. *stabilin1:YFP* were provided by Stefan Schulte-Merker, PhD of the Hubrecht Institute in the Netherlands. The reduced pigment *Casper* line was obtained from Leonard Zon, PhD of Harvard Medical School.

REFERENCES

1. Tammela, T, K Alitalo: Lymphangiogenesis: Molecular mechanisms and future promise. *Cell* 140 (2010), 460-476.
2. Alitalo, K, T Tammela, TV Petrova: Lymphangiogenesis in development and human disease. *Nature* 438 (2005), 946-953.
3. Shin, WS, SG Rockson: Animal models for the molecular and mechanistic study of lymphatic biology and disease. *Ann. NY Acad. Sci.* 1131 (2008), 50-74.
4. Sabin, FR: The lymphatic system in human embryos, with consideration of the morphology of the system as a whole. *Am. J. Anat.* 9 (1909), 43-91.
5. Kuchler, AM, E Gjini, J Peterson-Maduro, et al: Development of the zebrafish lymphatic system requires VEGFC signaling. *Curr. Biol.* 16 (2006), 1244-1248.
6. Yaniv, K, S Isogai, D Castranova, et al: Live imaging of lymphatic development in the zebrafish. *Nat. Med.* 12 (2006), 711-716.
7. Flores, MVCJH, KE Crosier, PS Crosier: Visualization of embryonic lymphangiogenesis advances the use of the zebrafish model for research in cancer and lymphatic pathologies. *Dev. Dynam.* 239 (2010), 2128-2135.
8. Hogan, BM, FL Bos, J Bussmann, et al: Ccbe1 is required for embryonic lymphangiogenesis and venous sprouting. *Nat. Genet.* 4 (2009), 396-398.
9. Bussmann, J, FL Bos, A Urasaki, et al: Arteries provide essential guidance cues for lymphatic endothelial cells in the zebrafish trunk. *Development* 137 (2010), 2653-2657.
10. Hove, RWJR, RW Koster, AS Forouhar, et al: Intracardiac fluid forces are an essential epigenetic factor for embryonic cardiogenesis. *Nature* 421 (2003), 172-177.
11. Isogai, S, M Horiguchi, BM Weinstein: The vascular anatomy of the developing zebrafish: An atlas of embryonic and early larval development. *Dev. Biol.* 230 (2001), 278-301.
12. Isogai, S, J Hitomi, K Yaniv, et al: Zebrafish as a new animal model to study lymphangiogenesis. *Anat. Sci. Int.* 84 (2009), 102-111.
13. Ny, A, M Koch, M Schneider, et al: A genetic *Xenopus laevis* tadpole model to study lymphangiogenesis. *Nat. Med.* 11 (2005), 998-1004.
14. Ruznyak, IFM, G Szabo: *Lymphatics and the Lymph Circulation*. Oxford: Pergamon Press, 1960.
15. Flores, MV, KE Crosier, PS Crosier: Visualization of embryonic lymphangiogenesis advances the use of the zebrafish model for research in cancer and lymphatic pathologies. *Dev. Dynam.* 239 (2010), 2128-2135.
16. Alders, M, BM Hogan, E Gjini, et al: Mutations in CCBE1 cause generalized lymph vessel dysplasia in humans. *Nat. Genet.* 41 (2009), 1272-1274.
17. Hermans, K, F Claes, W Vandeveld, et al: Role of synectin in lymphatic development in zebrafish and frogs. *Blood* 116 (2010), 3356-3366.
18. Geudens, I, R Herpers, K Hermans, et al: Role of delta-like-4/Notch in the formation and wiring of the lymphatic network in zebrafish. *Arterioscler. Thromb. Vasc. Biol.* 30 (2010), 1695-1702.
19. Harvey, NL, RS Srinivasan, ME Dillard, et al: Lymphatic vascular defects promoted by Prox1 haploinsufficiency cause adult-onset obesity. *Nat. Genet.* 37 (2005), 1072-1081.
20. Del Giacco, L, A Pistocchi, A Ghilardi: Prox1b Activity is essential in zebrafish lymphangiogenesis. *PLoS One* 5 (2010), e13170.

Mikah Coffindaffer-Wilson, PhD
Dept. of Molecular & Cellular Physiology
University of Cincinnati College of Medicine
231 Albert Sabin Way
P.O. Box 670576
Cincinnati, OH 45267-0576, USA
Phone: (513)-803-1104
E-mail: mikah.coffindaffer@cchmc.org